frontiers | Frontiers in Chemistry

ORIGINAL RESEARCH
published: 09 June 2022
doi: 10.3389/fchem.2022.911201

Bioactive Bibenzyl Enantiomers From the Tubers of *Bletilla striata*

Mei Zhou[1,2†], *Sai Jiang*[1,3†], *Changfen Chen*[1], *Jinyu Li*[1,2], *Huayong Lou*[1,2], *Mengyun Wang*[3], *Gezhou Liu*[1], *Hanfei Liu*[1,2], *Ting Liu*[4]* and *Weidong Pan*[1,2]*

[1]School of Basic Medical Sciences/State Key Laboratory of Functions and Applications of Medicinal Plants, Guizhou Medical University, Guiyang, China, [2]The Key Laboratory of Chemistry for Natural Products of Guizhou Province and Chinese Academy of Sciences, Guiyang, China, [3]TCM and Ethnomedicine Innovation and Development International Laboratory, School of Pharmacy, Innovative Materia Medica Research Institute, Hunan University of Chinese Medicine, Changsha, China, [4]Guizhou Provincial Key Laboratory of Pharmaceutics, Guizhou Medical University, Guiyang, China

Six new bibenzyls (three pairs of enantiomers), bletstrins D–F (1–3), were isolated from the ethyl acetate-soluble (EtOAc) extract of tubers of *Bletilla striata* (Thunb.) Rchb f. Their structures, including absolute configurations, were determined by 1D/2D NMR spectroscopy, optical rotation value, and experimental electronic circular dichroism (ECD) data analyses, respectively. Compounds 1–3 possess a hydroxyl-substituted chiral center on the aliphatic bibenzyl bridge, which represented the first examples of natural bibenzyl enantiomers from the genus of *Bletilla*. The antibacterial, antitumor necrosis factor (anti-TNF-α), and neuroprotective effects of the isolates have been evaluated. Compounds 3a and 3b were effective against three Gram-positive bacteria with minimum inhibitory concentrations (MICs) of 52–105 μg/ml. Compounds 2a and 2b exhibited significant inhibitory effects on TNF-α-mediated cytotoxicity in L929 cells with IC_{50} values of 25.7 ± 2.3 μM and 21.7 ± 1.7 μM, respectively. Subsequently, the possible anti-TNF-α mechanism of 2 was investigated by molecular docking simulation. Furthermore, the neuroprotective activities were tested on the H_2O_2-induced PC12 cell injury model, and compounds 2b, 3a, and 3b (10 μM) could obviously protect the cells with the cell viabilities of 57.86 ± 2.08%, 64.82 ± 2.84%, and 64.11 ± 2.52%, respectively.

Keywords: ***Bletilla striata*, bibenzyl enantiomers, antibacterial, anti-TNF-α activity, neuroprotection**

OPEN ACCESS

Edited by:
Matthew A. Coleman, University of California, Davis, United States

Reviewed by:
Jungui Dai, Chinese Academy of Medical Sciences and Peking Union Medical College, China
Rufeng Wang, Shanghai University of Traditional Chinese Medicine, China

***Correspondence:**
Ting Liu
liuting@gmc.edu.cn
Weidong Pan
wdpan@163.com

[†]*These authors have contributed equally to this work*

Specialty section:
This article was submitted to Chemical Biology, a section of the journal Frontiers in Chemistry

Received: *02 April 2022*
Accepted: *02 May 2022*
Published: *09 June 2022*

Citation:
Zhou M, Jiang S, Chen C, Li J, Lou H, Wang M, Liu G, Liu H, Liu T and Pan W (2022) Bioactive Bibenzyl Enantiomers From the Tubers of Bletilla striata. Front. Chem. 10:911201. doi: 10.3389/fchem.2022.911201

INTRODUCTION

The tubers of *Bletilla striata* (Thunb.) Rchb. f, named "Bai Ji", is a traditional Chinese medicine, which are used for the treatment of several health disorders, including gastrointestinal disorders, ulcers, lung disorders, chapped skin, and traumatic bleeding (He et al., 2017; Zhang et al., 2019; Liao et al., 2019; Wang et al., 2020; Hou et al., 2021; Wang et al., 2021; Jiang et al., 2021; Xu et al., 2021). As an Orchidaceae plant, it can biosynthesize many secondary stilbenes, such as bibenzyls, phenanthrenes, dihydrophenanthrenes, biphenanthrenes, dihydrophenanthrofurans, and phenanthrenequinones (Sun et al., 2016; Jiang et al., 2019a; Zhu et al., 2021). Some of these compounds showed a wide range of biological activities like antibacterial, anti-inflammatory, neuroprotective, anticancer, and antiviral effects (Qian et al., 2015; Wang and Meng, 2015; Xu et al., 2019; Jiang et al., 2020; Jiang et al., 2021). In our previous work, more than 40 stilbenes including 13 new compounds were isolated from the tubers of *B. striata* and just tested for their antibacterial effects (Jiang et al., 2019a, Jiang et al., 2019b).

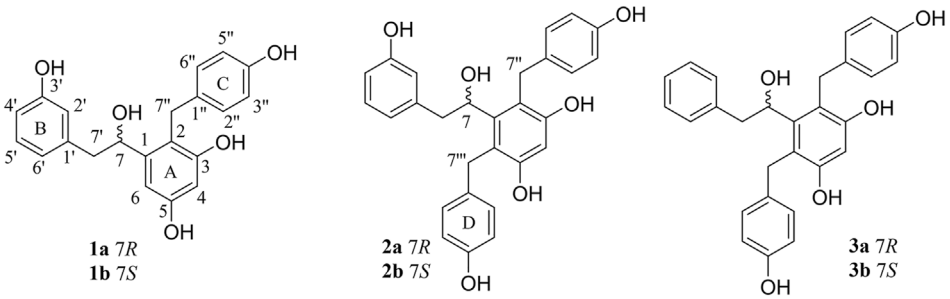

FIGURE 1 | Isolated compounds 1–3 from the tubers of *B. striata*.

Some literature studies showed that some compounds isolated from the tubers of *B. striata* presented obvious anti-neuroinflammatory activities (Sun et al., 2021), indicating that *B. striata* might be a promising source of neuroprotection lead compounds. The aim of this study was to obtain further chemical and biological properties of *B. striata*, which might provide deeper insights into the plant as a promising Chinese medicine. As a result, six new bibenzyls (three pairs of enantiomers), bletstrins D-F (1–3), were isolated (**Figure 1**). The isolation and identification of these undescribed compounds and their absolute configurations were elucidated in this study. Moreover, all the compounds were tested for their antibacterial, anti-TNF-α, and neuroprotective activities. The molecular docking experiment was further conducted to reveal the potential mechanism of anti-TNF-α activity.

MATERIALS AND METHODS

General Experimental Procedures

Optical rotations were measured on a Rudolph Autopol IV-T polarimeter equipped. The UV spectra were measured on an HP 8543E spectrometer. IR spectra were obtained on a Nicolet iS10 and an ICAN 9 FT-IR spectrometer with KBr pellets. ECD spectra were recorded with an Applied Photophysics Chirascan instrument. ^{1}D and ^{2}D NMR spectra were recorded on a Varian Inova 400 Hz NMR instrument or a Bruker Avance NEO 600 MHz spectrometer with tetramethylsilane (TMS) as the internal standard. The high-resolution electrospray ionization mass spectra (HRESIMS) were obtained on a Thermo Q-Exactive Focus mass spectrometer. All the solvents used were of analytical grade (Jiangsu Hanbang Science and Technology Co., Ltd.). Silica gel (300–400 mesh, Qingdao Haiyang Chemical Co., Ltd.), CHP20/P120 MCI gel (75–150 μm, Mitsubishi Chemical Industries, Ltd.), and Sephadex LH-20 (25–100 μm, Amersham Biosciences, Sweden) were used for column chromatography (CC). Semi-preparative HPLC was performed on a Waters-600 machine with a W2489 UV detector, column: ODS (5 μm, 10 × 250 mm, Waters Co., Ltd, United States). Chiral HPLC was performed on a Waters-600 machine with a W2489 UV detector equipped with a CHIRALPAK IA column (4.6 i. d. × 250 mm, S-5 μm, Daicel Chiral Technologies Co., Ltd., Japan). GF-254 (Qingdao Haiyang Chemical Co., Ltd.) was used for TLC.

Plant Material

The tubers of *B. striata* were collected from Anlong County of Guizhou Province, People's Republic of China, in March 2017, and authenticated by Prof. Ming-kai Wu (Institute of Modern Chinese Medicinal Materials, Guizhou Academy of Agricultural Sciences, Guizhou). A voucher specimen (No. 20170312003) was deposited at the State Key Laboratory of Functions and Applications of Medicinal Plants, Guizhou Medical University, People's Republic of China.

Extraction and Isolation

The dried tubers of *B. striata* (9.8 kg) were extracted with 95% ethyl alcohol (EtOH) under reflux four times to produce the crude extract. The residue was suspended in water and subsequently separated with EtOAc to yield an EtOAc-soluble fraction (386.1 g). The extract was purified on a silica gel column and eluted with a gradient $CHCl_3$-CH_3OH solvent system (100: 1→0:1) to give 11 fractions (Frs. 1–11). Frs. 5 (25.2 g) was separated by MCI CC eluted with H_2O-CH_3OH (from 60:0 to 0:100) to yield nine subfractions (Frs. 5.1–5.9). Frs. 5.5 (1.3 g) was further separated on a silica gel column and eluted with petroleum ether (PE)-EtOAc (10:1 to 1:1) to give five subfractions (Frs. 5.5.1–5.5.5). Frs. 5.5.4 (113.2 mg) was purified by semi-preparative HPLC (CH_3OH-H_2O, 56:44, flow rate 2.0 ml/min) to afford three subfractions (16.8 mg, t_R = 19.61 min). Frs. 5.5.5 (238.6 mg) was purified by semi-preparative HPLC (CH_3OH-H_2O, 56:44, flow rate 2.0 ml/min) to afford three subfractions (5.4 mg, t_R = 31.63 min). Frs. 5.6 (756.3 mg) was subjected to being chromatographed on a silica gel column and eluted with PE-EtOAc (10:1 to 1:1) to give three subfractions (Frs. 5.6.1–5.6.3). Frs. 5.6.3 (86.4 mg) was purified by semi-preparative HPLC (CH_3OH-H_2O, 55:45, flow rate 2.0 ml/min) to afford 1 subfraction (7.6 mg, t_R = 24.52 min). Compounds 1–3 were further purified by chiral HPLC, using CH_3OH-H_2O (50:50) as the mobile phase, to yield 1a (2.2 mg), 1b (2.8 mg), 2a (1.60 mg), 2b (1.85 mg), 3a (6.38 mg), and 3b (5.58 mg).

Bletstrin D (1) racemic mixture. Yellowish amorphous powder; UV (MeOH) λ_{max} (log ε) 280 (3.49) nm; IR (KBr):

TABLE 1 | ^{1}H and ^{13}C NMR data of compounds 1–3.

	1[a]		2[b]		3[c]	
No.	**δ_C**	**δ_H (*J* in Hz)**	**δ_C**	**δ_H (*J* in Hz)**	**δ_C**	**δ_H (*J* in Hz)**
1	146.7		144.0		144.0	
2	114.4		117.9		117.7	
3	155.7		155.3		155.4	
4	100.9	6.23, d (2.4)	103.0	6.43, s	102.7	6.45, s
5	156.1		156.9		156.9	
6	104.0	6.49, d (2.4)	118.8		118.8	
7	70.0	4.76, dd (10.8 and 6.0)	73.6	5.17, dd (8.8 and 4.8)	73.7	5.15, dd (9.2 and 4.4)
1′	141.2		142.4		140.9	
2′	116.3	6.58, m	117.4	6.41, m	130.5	6.72, m
3′	156.9		157.9		128.9	7.11, m
4′	112.7	6.55, m	113.7	6.53, m	126.8	7.08, m
5′	128.7	6.99, t (7.8)	129.9	6.94, m	128.9	7.11, m
6′	120.0	6.46, m	121.8	6.21, m	130.5	6.76, m
7′	45.3	2.47, d (6.0)	44.3	2.70, dd (13.6 and 8.8) 2.34, dd (13.6 and 4.8)	44.3	2.77, dd (13.6 and 9.2) 2.35, dd (13.6 and 4.4)
1″	131.8		134.3		134.3	
2″, 6″	128.9	6.89, d (8.4)	130.1	6.94, m	130.1	6.94, m
3″, 5″	114.8	6.60, d (8.4)	115.6	6.66, d (8.4)	115.6	6.67, m
4″	155.0		155.5		155.5	
7″	28.8	3.76, d (15.6) 3.68, d (15.6)	30.8	3.83, d (16.0) 3.69, d (16.0)	30.8	3.78, s
1‴			135.2		135.2	
2‴, 6‴			130.1	6.94, m	130.1	6.94, m
3‴, 5‴			115.9	6.66, d (8.4)	115.9	6.67, m
4‴			156.0		156.1	
7‴			31.6	4.56, d (16.0) 4.18, d (16.0)	31.7	4.57, d (15.6) 4.20, d (15.6)
1⁗						
2⁗, 6⁗						
3⁗, 5⁗						
4⁗						
7⁗						
3-OH		9.07, s				
5-OH		8.96, s				
7-OH		4.85, d (4.2)				
3′-OH		9.03, s or 9.16, s				
4″-OH		9.16, s or 9.03, s				

[a] *^{1}H (600 MHz) and ^{13}C (150 MHz) NMR, data on DMSO-d_6.*
[b] *^{1}H (400 MHz) and ^{13}C (100 MHz) NMR, data on methanol-d_4.*
[c] *^{1}H (400 MHz) and ^{13}C (100 MHz) NMR, data on methanol-d_4.*

ν_{max} = 3,374, 1,611, 1,513, 1,225, 1,145, 986, and 693 cm^{-1}; ^{1}H and ^{13}C NMR data (see **Table 1**; HRESIMS *m/z* 351.1241 $[M - H]^-$ (calcd. for $C_{21}H_{19}O_5$, 351.1232).

(7*R*)-bletstrin D (1a). $[\alpha]_D^{22}$ +18.3 (*c* 0.04, MeOH); ECD (MeOH) λ_{max} ($\Delta\varepsilon$) 206 (+2.97), 219 (−0.74), and 236 (+1.03) nm.

(7*S*)-bletstrin D (1b). $[\alpha]_D^{22}$ −2.1 (*c* 0.05, MeOH); ECD (MeOH) λ_{max} ($\Delta\varepsilon$) 206 (−2.24), 217 (+0.50), and 236 (−0.68) nm.

Bletstrin E (2) racemic mixture. Yellowish amorphous powder; UV (MeOH) λ_{max} (log ε) 280 (2.93) nm; IR (KBr): ν_{max} = 3,381, 1,595, 1,510, 1,457, 1,236, and 1,172 cm^{-1}; ^{1}H and ^{13}C NMR data (see **Table 1**); HRESIMS *m/z* 457.1664 $[M - H]^-$ (calcd. for $C_{28}H_{25}O_6$, 457.1651).

(7*R*)-bletstrin E (2a). $[\alpha]_D^{22}$ +12.5 (*c* 0.05, MeOH); ECD (MeOH) λ_{max} ($\Delta\varepsilon$) 202 (+6.49), 217 (−1.51), and 230 (+1.13) nm.

(7*S*)-bletstrin E (2b). $[\alpha]_D^{22}$ −4.5 (*c* 0.06, MeOH); ECD (MeOH) λ_{max} ($\Delta\varepsilon$) 201 (−3.97), 218 (+1.28), and 230 (−0.51) nm.

Bletstrin F (3) racemic mixture. Yellowish amorphous powder; UV (MeOH) λ_{max} (log ε) 285 (3.23) nm; IR (KBr): ν_{max} = 3,379, 1,599, 1,510, 1,238, 1,170, 1,083, and 702 cm^{-1}; ^{1}H and ^{13}C NMR data (see **Table 1**); HRESIMS *m/z* 443.1852 $[M + H]^+$ (calcd. for $C_{28}H_{27}O_5$, 443.1858).

(7*R*)-bletstrin F (3a). $[\alpha]_D^{22}$ +28.7 (*c* 0.05, MeOH); ECD (MeOH) λ_{max} ($\Delta\varepsilon$) 203 (+4.11), 219 (−1.07), and 231 (+1.35) nm.

(7*S*)-bletstrin F (3b). $[\alpha]_D^{22}$ −10.1 (*c* 0.05, MeOH); ECD (MeOH) λ_{max} ($\Delta\varepsilon$) 204 (−2.24), 219 (+1.38), and 231 (−0.54) nm.

Antibacterial Activity Assays

Antimicrobial activities of compounds 1–3 against Gram-positive bacteria (Methicillin-resistant *S. aureus* ATCC 43300, *S. aureus* ATCC 6538, and *Bacillus subtilis* ATCC 6051) and Gram-negative bacteria (*Escherichia coli* ATCC 11775) were performed using a microbroth dilution method in a 96-well

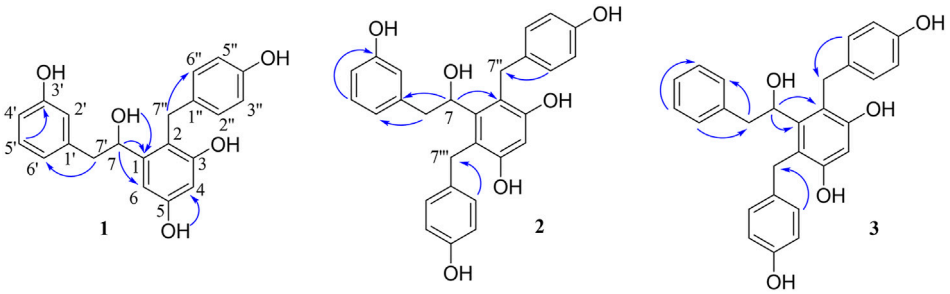

FIGURE 2 | Key HMBC correlations of compounds 1–3.

microtiter plate (Jiang, et al., 2019a). Bacteria were seeded at 1×10^6 cells per well (200 μL) in a 96-well plate containing Mueller-Hinton broth with different concentrations (from 1 to 420 μg/ml; 2-fold increments) of each test compound. Oxacillin, which was obtained from J&K Chemicals (Beijing, China), was used as a positive control.

Anti-TNF-α Activity Assay

L929 cells (Procell, Wuhan, China) were cultured in RPMI 1640 (Gibco, United States) supplemented with 10% fetal calf serum (Procell, Wuhan, China) at 37°C in a humidified atmosphere of 5% CO_2. Exponentially growing L929 cells were harvested and seeded in 96-well multiplates at a density of 1.5×10^5 cells/mL. After incubation for 24 h at 37°C, samples (0.01, 0.1, 10, 20, 40, 80, and 200 μM), TNF-α (GlpBio, Shanghai, China) (7.5 ng/ml), and actinomycin D (GlpBio, Shanghai, China) (0.5 μg/ml) were added. After 12 h incubation at 37°C, 100 μL of 3-(4,5-dimethylthiazol-2-yl)-5-2 -(4-sulfophenyl)-2H-tetrazolium (MTS) (Promega, United States) (0.5 mg/ml) was added to each well and incubated for an additional 2 h. The optical density (OD) of the formazan solution was measured using a microplate reader at 490 nm. UCB-9260 (GlpBio, Shanghai, China) was used as a positive control.

Neuroprotective Activity Assay

PC12 cells were cultured in Ham's F12K (Gibco, United States) with 10% fetal calf serum at 37°C in a humidified atmosphere of 5% CO_2. The cells were seeded in 96-well multiplates at a density of 1.5×10^5 cells/mL. After overnight incubation at 37°C with 5% CO_2, 10 μM test samples and H_2O_2 (final concentration of 450 μM) were added into the wells and incubated for another 12 h. The cell survival rate was measured by 3-(4,5-dimethylthiazol-2-yl)-2,5-diphenyltetrazolium bromide (MTT) (Gibco, United States) assay (Chu et al., 2019).

RESULTS AND DISCUSSION

Compound 1 was obtained as a yellowish amorphous powder. HRESIMS analysis established the molecular formula of 1 as $C_{21}H_{20}O_5$ (*m/z* 351.1241 $[M - H]^-$, calcd. 351.1232). The UV spectrum suggested the presence of aromatic ring functional groups. The ^{1}H NMR spectrum of 1 revealed signals for one 1,3-disubstituted phenyl group [δ_H 6,99 (1H, t, J = 7.8 Hz), 6.58 (1H, m), 6.55 (1H, m), and 6.46 (1H, m)]; one 4-hydroxybenzyl moiety [δ_H 6.89 (2H, d, J = 8.4 Hz), 6.60 (2H, d, J = 8.4 Hz), 3.76 (1H, d, J = 15.6 Hz), and 3.68 (1H, d, J = 15.6 Hz)]; one 1,2,3,5-tetrasubstituted aromatic moiety [δ_H 6.49 (1H, d, J = 2.4 Hz) and 6.23 (1H, d, J = 2.4 Hz)]; one methylene group [δ_H 2.47 (2H, d, J = 6.0 Hz)]; one oxymethine group [δ_H 4.22 (1H, dd, J = 10.8, 6.0 Hz)]; and four hydroxy groups [δ_H 9.16 (1H, s), 9.07 (1H, s), 8.96 (1H, s), and 4.85 (1H, d, J = 4.2 Hz)]. The ^{13}C NMR spectrum of 1 showed 21 signals, four of them were oxygen-bearing aromatic carbons (δ_C 156.9, 156.1, 155.7, and 155.0), and one of them was oxygen-bearing methylene group (δ_C 70.0). The 1D-NMR data of **1** were similar to those of bletstrin A (Jiang et al., 2019b), except for the existence of an extra hydroxy group linked to the C-3′ position. This conclusion was supported by the molecular weight and the HMBC (**Figure 2**) correlations of H-5′ (δ_H 6.99) and H-2′ (δ_H 6.58) to C-3′ (δ_C 156.9). Thus, the planar structure of **1** was established.

However, compound 1 was not optically pure but racemic according to its optical rotation data (Shao et al., 2019). We then separated optically pure compounds 1a and 1b from one by chiral HPLC. Compounds 1a and 1b exhibited opposite cotton effects at 206, 219, and 236 nm and further confirmed their racemic relationship. By comparison of the experimental ECD curves and data from the literature (Jiang et al., 2019b), the absolute configurations of 1a and 1b were determined as 7*R* and 7*S*, respectively. Finally, the structures of bletstrin D (1a and 1b) were defined. All the spectroscopic data of compound 1 are shown in **Supplementary Figures S1–8** in **Supplementary Material S1**.

Compound 2 was obtained as a yellowish amorphous powder. Its molecular formula of $C_{28}H_{26}O_6$ was determined by the (-)-HRESIMS ion peak at *m/z* 457.1644 $[M - H]^-$ (calcd. 457.1651). The comparison of the ^{1}D NMR data (**Table 1**) of 2 with those of 1 suggested that their structures were similar, except for the existence of an extra benzene moiety in 2. The ^{1}H NMR data of compound 2 showed an extra AA′BB' system benzene moiety at δ_H 6.94 (2H, m, H-2‴, 6‴), 6.66 (2H, d, J = 8.4 Hz, H-3‴, 5‴), 4.56 (1H, d, J = 16.0 Hz), and 4.18 (1H, d, J = 16.0 Hz) in the A ring. The ^{13}C NMR spectrum of compound 2 showed seven extra signals at δ_C 135.2 (C-1‴), 130.1 (C-2‴), 115.6 (C-3‴), 155.5 (C-4‴), 115.6 (C-5‴), 130.1 (C-6‴), and 31.6 (C-7‴). Furthermore, the HMBC (**Figure 2**) correlations from H-

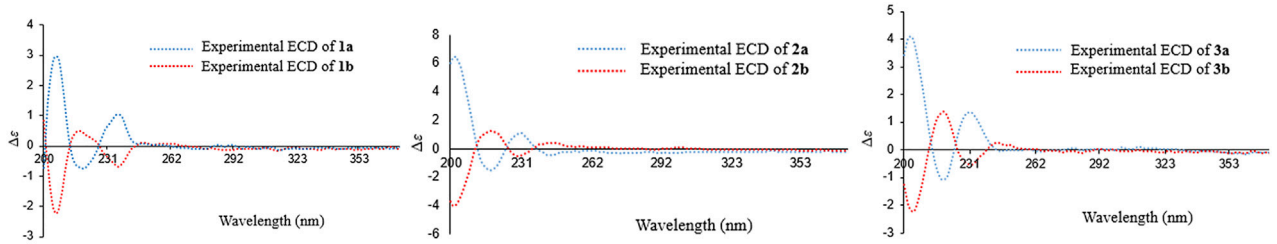

FIGURE 3 | Experimental ECD curves of compounds 1–3.

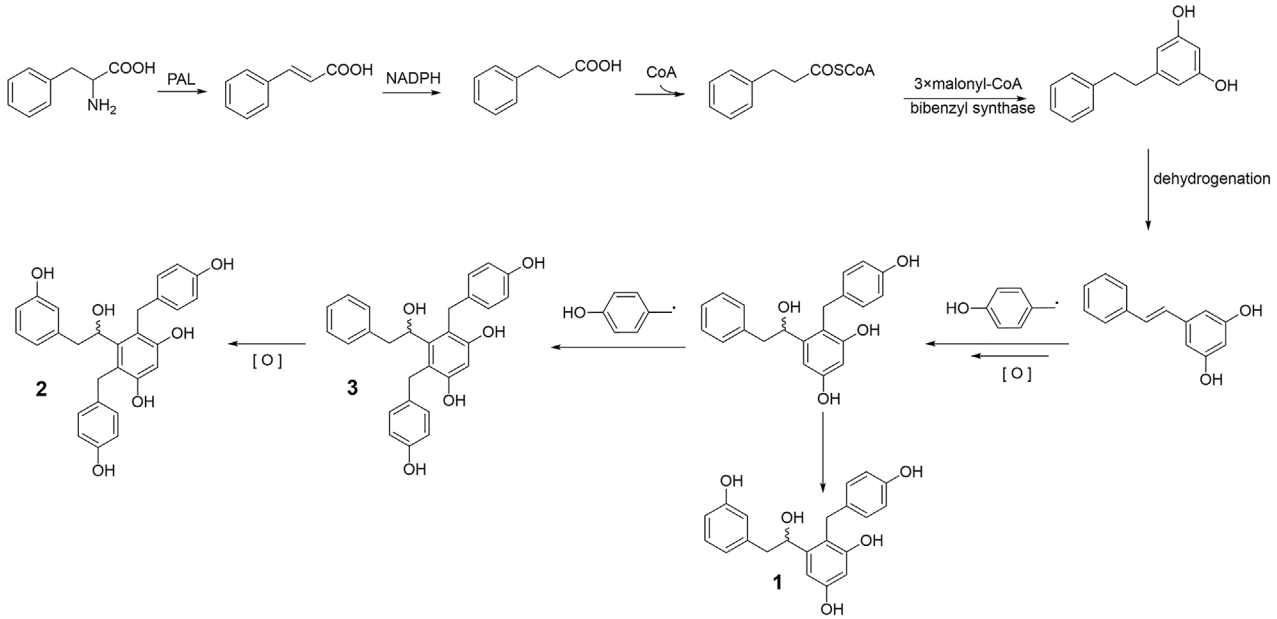

FIGURE 4 | Plausible biogenetic pathway of compounds 1–3.

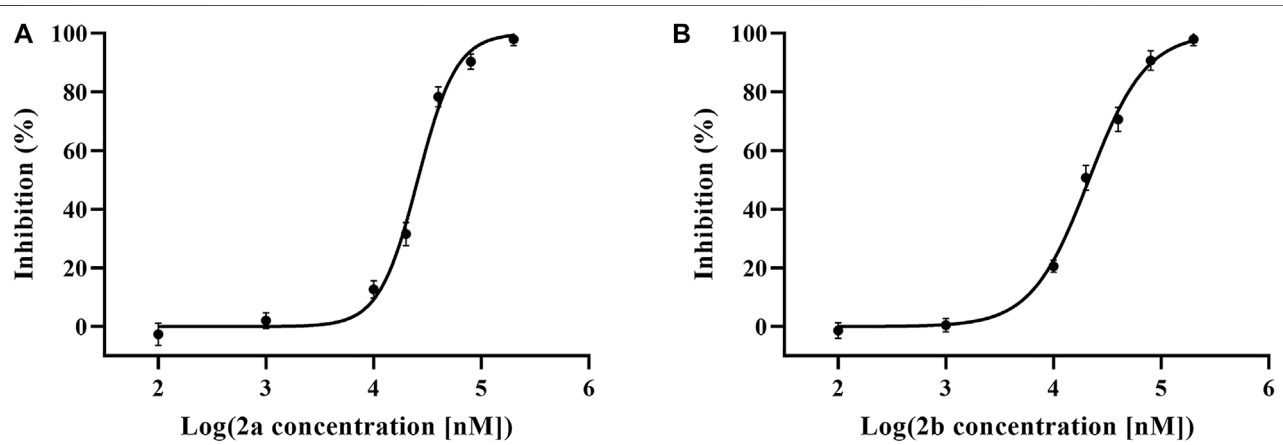

FIGURE 5 | L929 assay of compound 2 **(A,B)** in the presence of different concentrations (n = 3).

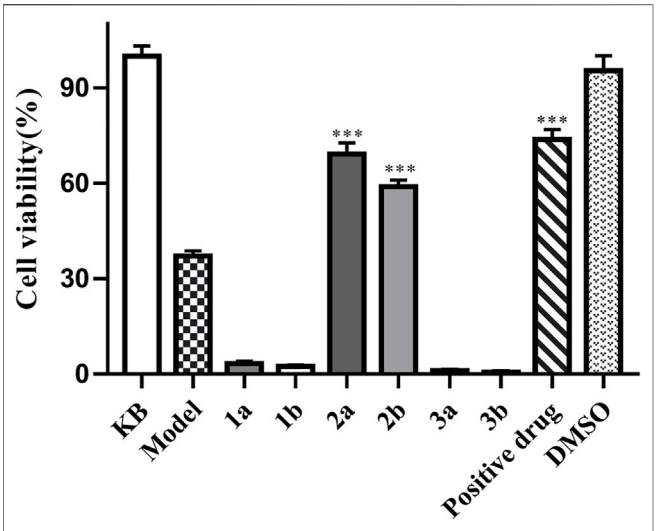

FIGURE 6 | Anti-TNF-α activities of compounds 1–3. L929 cells were cultured in the presence of isolated compounds and were measured by the MTS assay (n = 3). Data are expressed as mean ± S D. ***p < 0.001 vs. the model group.

7‴ (δ_H 4.56) to C-2‴, C‴, C-1, C-5, and C-6 suggested that the benzyl group was connected to C-6. Thus, the planar structure of 2 was defined and named as bletstrin E. Compound 2 was also a racemic mixture. Resolution by chromatography analysis is afforded to 2a and 2b. The absolute configurations of 2a and 2b were determined as 7*R* and 7*S* by comparing with the experimental ECD spectra of 1a and 1b. Finally, the structures of bletstrin E (2a and 2b) were defined. All the spectroscopic data on compound 2 are shown in **Supplementary Figures S8–16** in **Supplementary Material S1**.

Compound 3, a yellowish amorphous powder, was given the molecular formula of $C_{28}H_{26}O_5$ by (+)-HRESIMS ion peak at *m/z* 443.1852 $[M + H]^+$ (calcd. 443.1858). A comparison of the molecular formula of 3 with that of 2 inferred that it lacks an oxygen atom. By detailed analysis of the 1D NMR data (**Table 1**) of 3, it was suggested that its structure was similar to that of **2**, except for missing a hydroxy group at position C-3′. The location was supported by the downfield chemical shift of C-3′ at δ_C 128.9 ($\Delta\delta_C$ −29.0), as well as the HMBC (**Figure 2**) correlations of H-3′, 5′ (δ_H 7.11) with C-1′ (δ_C 140.9). Compound 3 was a racemate according to its optical rotation data. The pair of optically pure enantiomers (3a and 3b) was separated using chiral chromatography analysis. The absolute configurations of 3a and 3b were determined as 7*R* and 7*S* by comparing with the experimental ECD (**Figure 3**) spectra of 1a and 1b. Finally, the structures of bletstrin F (3a and 3b) were defined. All the spectroscopic data on compound 3 are shown in **Supplementary Figures S17–24** in **Supplementary Material S1**.

Bletstrins D–F (1–3) are all new bibenzyl derivatives possessing a rare hydroxyl substituted chiral center on the aliphatic bibenzyl bridge structure. In the field of a biosynthetic pathway, the establishment of the new structures may consist of a series of modifications from simple model blocks (Sun et al., 2021). As shown in **Figure 4**, bibenzyls are biosynthesized from dihydro-m-coumaroyl-CoA (Jiang et al., 2019). Subsequently, the target compounds 1, 2, and 3 were formed by dehydrogenation, oxidation, and the coupling of one or two benzyl groups.

Compounds 1–3 were tested on antibacterial activities against three common Gram-positive bacterial strains (Methicillin-resistant *Staphylococcus aureus* ATCC 43300, *S. aureus* ATCC 6538, and *Bacillus subtilis* ATCC 6051) and one Gram-negative bacterial strain (*Escherichia coli* ATCC 11775). The results revealed that compounds 3a and 3b were effective against three Gram-positive bacteria with MICs of 52–105 μg/ml (**Supplementary Table S1** in

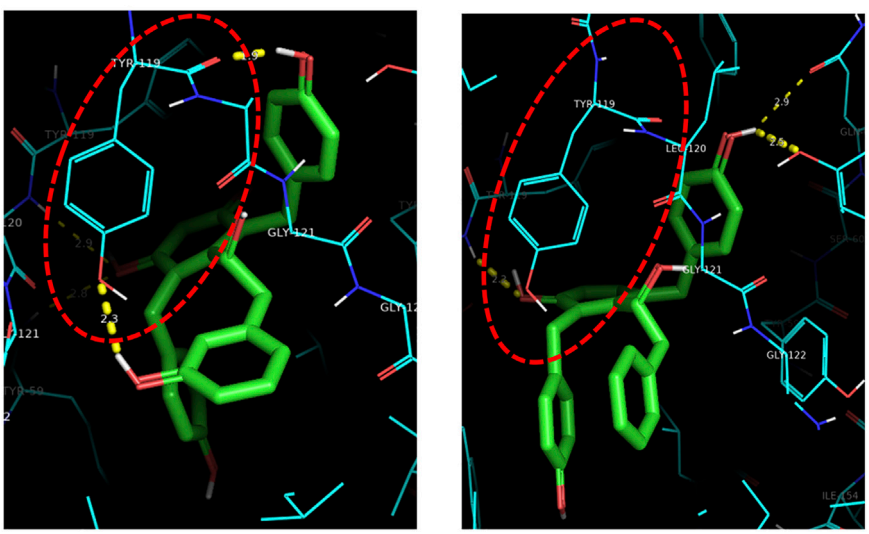

FIGURE 7 | Three-dimensional molecular docking model of compounds 2 and 3. Detail of the compound-binding pocket within the TNF homotrimer, with key residues involved in binding highlighted.

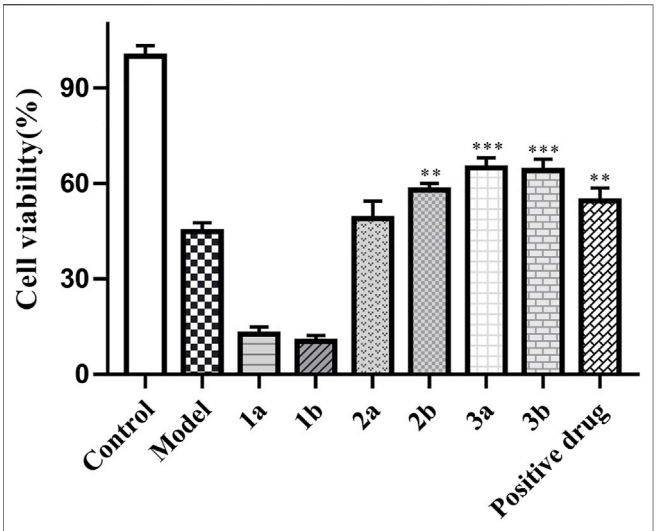

FIGURE 8 | Neuroprotective activities of compounds 1–3. PC12 cells were in the presence of isolated compounds at a concentration of 10 μM with the H_2O_2-induced injury model. Their cell viabilities were measured by the MTT assay (n = 3). Data are expressed as mean ± S D. ***$p < 0.001$ vs. the model group.

Supplementary Material S1). Furthermore, compounds 2a and 2b exhibited obvious anti-TNF-α bioactivity in TNF-α-mediated-cytotoxicity assay with IC_{50} values of 25.7 ± 2.3 μM and 21.7 ± 1.7 μM, respectively (**Figure 5**); these values are of the same order of magnitude to the published literature (He et al., 2005; Alexiou et al., 2014; Melagraki et al., 2017). The cell viability of 69.17 ± 2.42% and 58.89 ± 2.08% at 20 μM, compared to the model group (37.08 ± 1.68%), while that of the positive control UCB-9260 was 73.70 ± 3.12% (**Figure 6**). TNF-α is a proinflammatory cytokine that plays a key role in most of the inflammatory processes (Jacobi et al., 2006), and these results suggested that compounds 2a and 2b may have obvious anti-inflammatory activity. In the anti-TNF-α activity test, compound 2, which possesses one more hydroxy group than compound 3 at C-4′, showed significantly different activities (P < 0.001). The possible anti-TNF-α mechanisms of 2 and 3 were investigated by molecular docking simulation (**Figure 7**). From the docking mode of two compounds with TNF-α protein (PDB ID: 6OOY), it can be seen that compound 2 with hydroxy group at C-4′ can form two stable hydrogen bonds with 6OOY tyrosine at position 119 (tyrosine; Tyr), which could not be found in the docking model of 3 and 6OOY. In the published study on the crystal structure of 6OOY, it was also demonstrated that the ligand binds to the protein at position 119 of the B chain (O'Connell et al., 2019). This docking simulation revealed that compound 2 might form hydrogen bonds with amino acids at position 119 of the B chain of TNF-α, which can inhibit its activity by stabilizing the asymmetric trimer structure of TNF-α.

Moreover, *in vitro* assays, compounds 2b, 3a, and 3b (10 μM) exhibited excellent neuroprotective activities against H_2O_2-induced PC12 cell damage with the cell viabilities of 57.86 ± 2.08%, 64.82 ± 2.84%, and 64.11 ± 2.52%, respectively, while that of the positive control (±) α-Tocopherol was 54.51 ± 2.87% (**Figure 8**).

CONCLUSION

Six new bibenzyls (three pairs of enantiomers, 1a–3b) were isolated from the tubers of *B. striata*. The absolute configurations of compounds 1–3 were assigned by comparison of the optical rotation value combined with their experimental ECD data. All the compounds were evaluated for their antibacterial activities, but only compound 3 showed inhibitory activities against the three Gram-positive bacteria. This result preliminarily inferred that the orientation of hydroxyl at C-7 may not affect the antibacterial activities. Furthermore, the anti-TNF-α activity was influenced by the hydroxyl at C-4′ and the benzyl at C-6 by comparing the effects of 1, 2, and 3. Moreover, the absolute configurations may also not affect their neuroprotective activities, but the benzyl group at C-6 may affect their activity. In fact, this is the first example of natural bibenzyl enantiomers (a hydroxyl-substituted chiral center on the aliphatic bibenzyl bridge) from the genus of *Bletilla*. Furthermore, the anti-TNF-α and neuroprotective effects of bibenzyls from *B. striata* are also the first reported. In addition, some simple bibenzyls (not containing extra benzyl groups) from *Stemona* and *Dendrobium* species also showed neuroprotective activities against 6-hydroxydopamine-induced neurotoxicity in human neuroblastoma SH-SY5Y cells (Lee et al., 2006; Song et al., 2010). In summary, according to the structure and activity relationship (SAR), the hydroxyl on the aliphatic chain and/or benzyl groups, as well as the absolute configurations, may affect the bioactivities of bibenzyls.

DATA AVAILABILITY STATEMENT

The original contributions presented in the study are included in the article/**Supplementary Material**; further inquiries can be directed to the corresponding authors.

AUTHOR CONTRIBUTIONS

WP and TL conceived and designed the experiment. MZ and CC were responsible for compound isolation and writing. JS was responsible for structure identification. HL, MW, and GL completed the biological activity test. JL and HL reviewed the manuscript. All authors have read and agreed to the final manuscript.

FUNDING

This work was financially supported by the National Nature Science Foundation of China (Nos. U1812403-3-2, 81660580, and 32100322) and the Science and Technology Department of Guizhou Province (Nos. QKHZC(2019)2753, QKHZC(2020) 4Y067, QKHRC(2016)4037, and QKHPTRC(2021)5619).

SUPPLEMENTARY MATERIAL

The Supplementary Material for this article can be found online at: https://www.frontiersin.org/articles/10.3389/fchem.2022.911201/full#supplementary-material

REFERENCES

Alexiou, P., Papakyriakou, A., Ntougkos, E., Papaneophytou, C. P., Liepouri, F., Mettou, A., et al. (2014). Rationally Designed Less Toxic SPD-304 Analogs and Preliminary Evaluation of Their TNF Inhibitory Effects. *Arch. Pharm. Chem. Life Sci.* 347, 798–805. doi:10.1002/ardp.201400198

Chu, Q., Chen, M., Song, D., Li, X., Yang, Y., Zheng, Z., et al. (2019). Apios Americana Medik Flowers Polysaccharide (AFP-2) Attenuates H2O2 Induced Neurotoxicity in PC12 Cells. *Int. J. Biol. Macromol.* 123, 1115–1124. doi:10.1016/j.ijbiomac.2018.11.078

He, M. M., Smith, A. S., Oslob, J. D., Flanagan, W. M., Braisted, A. C., Whitty, A., et al. (2005). Small-Molecule Inhibition of TNF-α. *Science* 310, 1022–1025. doi:10.101126/science.111630410.1126/science.1116304

He, X., Wang, X., Fang, J., Zhao, Z., Huang, L., Guo, H., et al. (2017). Bletilla Striata: Medicinal Uses, Phytochemistry and Pharmacological Activities. *J. Ethnopharmacol.* 195, 20–38. doi:10.1016/j.jep.2016.11.026

Hou, X.-Y., Cao, Y., Wu, B.-L., Chen, B., Li, F., Wang, F., et al. (2021). New 2-isobutylmalates from the Tubers of *Bletilla Striata* and Their Potential Anti-pulmonary Fibrosis Activities. *Phytochem. Lett.* 46, 95–99. doi:10.1016/j.phytol.2021.09.009

Jacobi, A., Mahler, V., Schuler, G., and Hertl, M. (2006). Treatment of Inflammatory Dermatoses by Tumour Necrosis Factor Antagonists. *J. Eur. Acad. Dermatol Venerol.* 20 (10), 1171–1187. doi:10.1111/j.1468-3083.2006.01733.x

Jiang, S., Chen, C.-F., Ma, X.-P., Wang, M.-Y., Wang, W., Xia, Y., et al. (2019a). Antibacterial Stilbenes from the Tubers of *Bletilla Striata*. *Fitoterapia* 138, 104350. doi:10.1016/j.fitote.2019.104350

Jiang, S., Wan, K., Lou, H.-Y., Yi, P., Zhang, N., Zhou, M., et al. (2019b). Antibacterial Bibenzyl Derivatives from the Tubers of Bletilla Striata. *Phytochemistry* 162, 216–223. doi:10.1016/j.phytochem.2019.03.2210.1016/j.phytochem.2019.03.022

Jiang, S., Wang, M., Jiang, L., Xie, Q., Yuan, H., Yang, Y., et al. (2021). The Medicinal Uses of the Genus *Bletilla* in Traditional Chinese Medicine: A Phytochemical and Pharmacological Review. *J. Ethnopharmacol.* 280, 114263. doi:10.1016/j.jep.2021.114263

Jiang, S., Wang, M. Y., Yuan, H. W., Xie, Q., Liu, Y., Jian, Y. Q., et al. (2020). Medicinal Plant of *Bletilla Striata:* A Review of its Chemical Constituents, Pharmacological Activities, and Quality Control. *World J. Tradit. Chin. Med.* 6, 393–407. doi:10.4103/wjtcm.wjtcm5820

Lee, K. Y., Sung, S. H., and Kim, Y. C. (2006). Neuroprotective Bibenzyl Glycosides of *Stemona Tuberosa* Roots. *J. Nat. Prod.* 69, 679–681. doi:10.1021/np0504154

Liao, Z., Zeng, R., Hu, L., Maffucci, K. G., and Qu, Y. (2019). Polysaccharides from Tubers of *Bletilla Striata*: Physicochemical Characterization, Formulation of Buccoadhesive Wafers and Preliminary Study on Treating Oral Ulcer. *Int. J. Biol. Macromol.* 122, 1035–1045. doi:10.1016/j.ijbiomac.2018.09.050

Melagraki, G., Ntougkos, E., Rinotas, V., Papaneophytou, C., Leonis, G., Mavromoustakos, T., et al. (2017). Cheminformatics-aided Discovery of Small-Molecule Protein-Protein Interaction (PPI) Dual Inhibitors of Tumor Necrosis Factor (TNF) and Receptor Activator of NF-κB Ligand (RANKL). *PLoS Comput. Biol.* 13, e1005372. doi:10.1371/journal.pcbi.1005372

O'Connell, J., Porter, J., Kroeplien, B., Norman, T., Rapecki, S., Davis, R., et al. (2019). Small Molecules that Inhibit TNF Signalling by Stabilising an Asymmetric Form of the Trimer. *Nat. Commun.* 10, 5795–5805. doi:10.1038/s41467-019-1316-110.1038/s41467-019-13616-1

Qian, C.-D., Jiang, F.-S., Yu, H.-S., Shen, Y., Fu, Y.-H., Cheng, D.-Q., et al. (2015). Antibacterial Biphenanthrenes from the Fibrous Roots of *Bletilla Striata*. *J. Nat. Prod.* 78, 939–943. doi:10.1021/np501012n

Shao, S.-Y., Wang, C., Han, S.-W., Sun, M.-H., and Li, S. (2019). Phenanthrenequinone Enantiomers with Cytotoxic Activities from the Tubers of *Pleione Bulbocodioides*. *Org. Biomol. Chem.* 17, 567–572. doi:10.1039/C8OB02850H

Song, J.-X., Shaw, P.-C., Sze, C.-W., Tong, Y., Yao, X.-S., Ng, T.-B., et al. (2010). Chrysotoxine, a Novel Bibenzyl Compound, Inhibits 6-hydroxydopamine Induced Apoptosis in SH-SY5Y Cells via Mitochondria Protection and NF-κB Modulation. *Neurochem. Int.* 57, 676–689. doi:10.1016/j.neuint.2010.08.007

Sun, A., Liu, J., Pang, S., Lin, J., and Xu, R. (2016). Two Novel Phenanthraquinones with Anti-cancer Activity Isolated from Bletilla Striata. *Bioorg. Med. Chem. Lett.* 26, 2375–2379. doi:10.1016/j.bmcl.2016.01.076

Sun, M.-H., Ma, X.-J., Shao, S.-Y., Han, S.-W., Jiang, J.-W., Zhang, J.-J., et al. (2021). Phenanthrene, 9,10-dihydrophenanthrene and Bibenzyl Enantiomers from *Bletilla Striata* with Their Antineuroinflammatory and Cytotoxic Activities. *Phytochemistry* 182, 112609. doi:10.1016/j.phytochem.202011260910.1016/j.phytochem.2020.112609

Wang, B., Zhang, H., Chen, L., Mi, Z., Xu, Y., Zhao, G., et al. (2020). Extraction, Purification, and Determination of the Gastroprotective Activity of Glucomannan from *Bletilla Striata*. *Carbohydr. Polym.* 246, 116620. doi:10.1016/j.carbpol.202011662010.1016/j.carbpol.2020.116620

Wang, W., and Meng, H. (2015). Cytotoxic, Anti-inflammatory and Hemostatic Spirostane-Steroidal Saponins from the Ethanol Extract of the Roots of *Bletilla Striata*. *Fitoterapia* 101, 12–18. doi:10.16/j.fitote.2014.11.00510.1016/j.fitote.2014.11.005

Wang, X., Xing, M., Zhang, Z., Deng, L., Han, Y., Wang, C., et al. (2021). Using UPLC-QTOF/MS and Multivariate Analysis to Explore the Mechanism of *Bletilla Striata* Improving PM2.5-induced Lung Impairment. *Anal. Biochem.* 631, 114310. doi:10.1016/j.ab.2021.114310

Xu, D., Pan, Y., and Chen, J. (2019). Chemical Constituents, Pharmacologic Properties, and Clinical Applications of Bletilla Striata. *Front. Pharmacol.* 10, 1168–1186. doi:10.3389/fphar.2019.01168

Xu, J., Chen, Z., Liu, P., Wei, Y., Zhang, M., Huang, X., et al. (2021). Structural Characterization of a Pure Polysaccharide from Bletilla Striata Tubers and its Protective Effect against H2O2-Induced Injury Fibroblast Cells. *Int. J. Biol. Macromol.* 193, 2281–2289. doi:10.16/j.biomac.2021.11.06010.1016/j.ijbiomac.2021.11.060

Zhang, C., Gao, F., Gan, S., He, Y., Chen, Z., Liu, X., et al. (2019). Chemical Characterization and Gastroprotective Effect of an Isolated Polysaccharide Fraction from *Bletilla Striata* against Ethanol-Induced Acute Gastric Ulcer. *Food Chem. Toxicol.* 131, 110539. doi:10.1016/j.fct.2019.0504710.1016/j.fct.2019.05.047

Zhu, H., Dai, O., Zhou, F., Yang, L., Liu, F., Liu, Y., et al. (2021). Discovery of Bletillain, an Unusual Benzyl Polymer with Significant Autophagy-Inducing Effects in A549 Lung Cancer Cells through the Akt/GSK-3β/β-Catenin Signaling Pathway. *Bioorg. Chem.* 117, 105449. doi:10.1016/j.bioorg.2021.105449

Conflict of Interest: The authors declare that the research was conducted in the absence of any commercial or financial relationships that could be construed as a potential conflict of interest.

Publisher's Note: All claims expressed in this article are solely those of the authors and do not necessarily represent those of their affiliated organizations, or those of the publisher, the editors, and the reviewers. Any product that may be evaluated in this article, or claim that may be made by its manufacturer, is not guaranteed or endorsed by the publisher.